JACS
JOURNAL OF THE AMERICAN CHEMICAL SOCIETY

Communication

pubs.acs.org/JACS

Self-Assembled PbSe Nanowire:Perovskite Hybrids

Zhenyu Yang,[‡] Emre Yassitepe,[‡] Oleksandr Voznyy, Alyf Janmohamed, Xinzheng Lan, Larissa Levina, Riccardo Comin, and Edward H. Sargent*

The Edward S. Rogers Department of Electrical and Computer Engineering, University of Toronto, 10 King's College Road, Toronto, Ontario M5S 3G4, Canada

Supporting Information

ABSTRACT: Inorganic semiconductor nanowires are of interest in nano- and microscale photonic and electronic applications. Here we report the formation of PbSe nanowires based on directional quantum dot alignment and fusion regulated by hybrid organic−inorganic perovskite surface ligands. All material synthesis is carried out at mild temperatures. Passivation of PbSe quantum dots was achieved via a new perovskite ligand exchange. Subsequent *in situ* ammonium/amine substitution by butylamine enables quantum dots to be capped by butylammonium lead iodide, and this further drives the formation of a PbSe nanowire superlattice in a two-dimensional (2D) perovskite matrix. The average spacing between two adjacent nanowires agrees well with the thickness of single atomic layer of 2D perovskite, consistent with the formation of a new self-assembled semiconductor nanowire:perovskite heterocrystal hybrid.

Colloidal quantum dots (CQDs) are of interest in view of their distinctive quantum-confined physical and chemical properties.[1−4] Anisotropic growth of CQDs into one-dimensional (1D) nanostructures, such as nanorods and nanowires, breaks the particles' spherical or pseudospherical symmetry.[5,6] This directional growth further enriches the diversity of semiconductor nanostructures and significantly broadens semiconductor application areas to include light emitters,[7] field-effect transistors,[8,9] biosensors,[10,11] and photovoltaics.[12]

Anisotropic growth of 1D structures can be achieved through several kinetically promoted methods, such as seed-directed growth,[6] catalysis-driven assembly,[13] and self-assembly of CQDs.[14] In contrast with other methods, self-assembly enables original CQD building blocks to align spontaneously to form desirable 1D structures; it does not require additional precursors or surfactants. However, CQD self-assembly requires precise control over many factors including solvent, concentration, surface energy, ligand type, temperature, and method of processing.[15−19] Reports have demonstrated CQD network fabricated via 2D self-assembly; however, similar methods have failed to yield 1D structures if no strong external driving force, such as high pressure and heat, is applied.[14,20] A general and facile approach to fabricate CQD self-assembled 1D structures is of considerable interest as a result.

In addition to being enabled by strong forces (e.g., surface charge polarization),[14,21] CQD self-assembly can be also achieved by weak intermolecular interactions such as van der Waals force among ligands.[22,23] Inspired by the recent finding of surface passivation[24−26] and coherent growth of methylammonium lead triiodide ($MAPbI_3$) perovskite ligands on CQD surfaces,[27,28] we pursued ligand-driven self-assembly with the goal of obtaining PbSe nanowires. The methodology is summarized in Figure 1a. An optimized two-step ligand exchange method enables CQDs to be passivated via a hybrid perovskite ligand, butylammonium lead tetraiodide ($(BA)_2PbI_4$). Spontaneous assembly of BA organic chains can be used to cross-link and thus crystallize to form perovskite as the spacer among CQDs, thereby regulating the alignment among CQDs. To the best of our knowledge, this represents

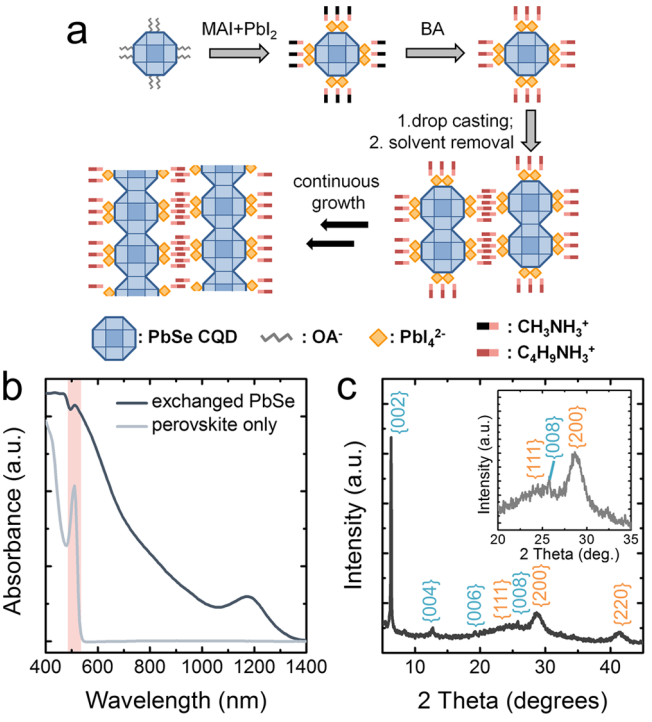

Figure 1. (a) Synthetic pathway from OA-capped PbSe CQDs to PbSe nanowire:perovskite self-assembled hybrids. (b) Absorption spectra of exchanged perovskite-passivated PbSe CQD films and control 2D perovskite sample. The characteristic peak at ∼510 nm is highlighted. (c) XRD pattern of perovskite-passivated PbSe CQD films. Crystal signals assigned perovskite and PbSe are labeled in blue and orange, respectively. Inset: Zoom-in of the XRD plot (2θ between 20° and 35°); the broad peak at 23°−32° is assigned to the glass substrate.

Received: October 11, 2015

DOI: 10.1021/jacs.5b10641
J. Am. Chem. Soc. XXXX, XXX, XXX−XXX

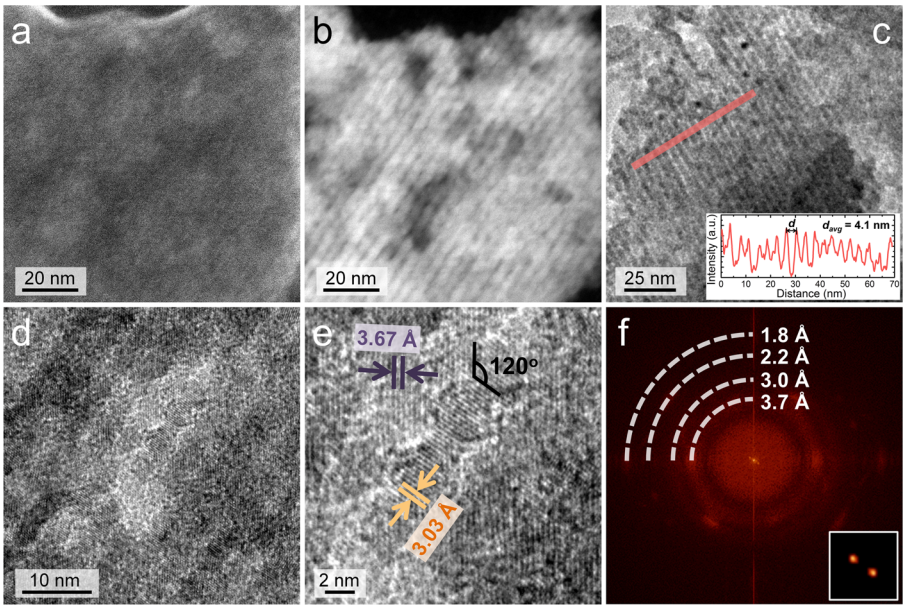

Figure 2. Electron microscopy analysis of PbSe:perovskite self-assembled heterocrystals. (a) SEM and (b) STEM-HAADF images of an individual heterocrystal. (c, d) Bright-field TEM images of self-assembled heterocrystals showing different contrast from PbSe and perovskite domains. Inset: Measurement of average distance between two adjacent nanowires (sample scanning line highlighted in red). (e) Zoom-in region of the center part of (d). (f) False color FFT of (d). Inset: FFT component (d = 4.1 nm, close to the center of (f)) assigned to superlattice pattern.

the first report of 1D self-assembly and growth of CQDs at mild temperatures within a solid-state matrix.

We prepared PbSe:perovskite hybrid crystals by drop-casting perovskite-ligand-passivated PbSe CQDs. PbSe CQDs were synthesized following an optimized hot injection method (see Supporting Information) and had diameter 2.7 ± 0.2 nm (Figure S1). A solution-based $MAPbI_3$ perovskite ligand exchange and subsequent washing process produced PbSe surfaces passivated by perovskite precursors. The particles were then highly soluble in polar solvents, such as butylamine, and dispersing them in such solvents produced a dark solution (8.8 mg/mL). When compared to the absorption spectrum of original oleic acid (OA)-capped CQDs, only a slight PL redshift (<30 nm) was observed, suggesting that the MAI + PbI_2 exchange provides good surface passivation. We also observed that MA^+ can be substituted using BA when BA is in excess. We conclude that surface 3D perovskite ligands (i.e., $MAPbI_3$) are gradually replaced with 2D perovskite ligands $(BA)_2PbI_4$. The absence of the $MAPbI_3$ structure is confirmed by absorption spectroscopy (Figure 1b): Once exchanged CQDs are deposited onto a glass substrate and annealed at 70 °C under nitrogen atmosphere, no PL signal is detected from this film sample. Instead of observing $MAPbI_3$, with its characteristic broad absorption peak (350−780 nm), we observe only contributions from PbSe and 2D perovskite in the resulting spectrum (Figure 1b): The broad signal from 1100 to 1220 nm corresponds to CQD absorption, while another absorption signal at ∼510 nm is consistent with the characteristic absorption of $(BA)_2PbI_4$ 2D perovskite (Figure 1b).

Consistent with the absorption features, 2D perovskite crystal signals are also present in X-ray diffraction (XRD) patterns (Figure 1c). No 3D perovskite crystalline signals are found, suggesting that MA^+/BA substitution is complete. The insertion of BA organic chains expands the d-spacing between two adjacent perovskite (00l) lattice planes, causing the selected crystal growth of the planar lattice layer. The corresponding narrow and strong signals arising from (00l) reflections are evident and indicate the formation of large 2D perovskite crystal domains. Similar patterns can be found in the published XRD results of crystals of $(BA)_2PbI_4$ (Figure S2).[29,30] PbSe nanocrystalline features at 2θ = 25°, 29°, and 41° are assigned to {111}, {200}, and {220} lattice planes, respectively.[31] Compared to the relatively weak {111} signal, the observation of strong {200} peak suggests the oriented alignment of PbSe nanocrystals within the film sample.

We now turn our attention to more detailed examination of the PbSe:perovskite hybrids using electron microscopy. Secondary electron microscopy (Figure 2a) confirms the presence of large grains with size over 200 nm. Only a small fraction of free-standing PbSe CQDs are observed. Scanning transmission electron microscopy high-angle annular dark-field (STEM-HAADF) imaging of the same square-shaped grains (Figure 2b) shows uniform 1D alignment of PbSe CQDs (higher contrast) residing inside the solid-state matrix (lower contrast). Similar wire-in-matrix structures are abundant on the sample grid (Figure S3). Transmission electron microscopy confirms that these wires align through the entire matrix with a uniform diameter (∼2.7 nm) along the observable length (Figure 2c), consistent with the original CQD diameter. The average center-to-center distance between two adjacent wires is 4.1 nm (Figure 2c inset). This value agrees well with the diameter of PbSe particles (2.7−2.8 nm) plus two-ended {100} parallel facets passivated by $(BA)PbI_4^-$ ligands (∼0.7 nm in length for single $(BA)PbI_4^-$ anion).

High-resolution TEM investigations provide valuable information about the crystal structure of the PbSe:perovskite hybrids (Figure 2d,e). The {200} PbSe atomic plane spacing (3.03 Å) is seen in the nanowire domains, suggesting that these aligned nanowires are formed by fusion of CQDs along the [100] direction. Another set of atomic plane spacings (3.67 Å) is seen across the entire image (Figure 2d) and more clearly shown in the gap between adjacent nanowires (Figure 2e). The value cannot be assigned to particular lattice plane from either PbSe, PbI_2, or $MAPbI_3$ crystals. Based on the d-spacing data of

DOI: 10.1021/jacs.5b10641
J. Am. Chem. Soc. XXXX, XXX, XXX−XXX

reported $(BA)_2PbI_4$ crystal structure (Figures S2)[26] and the PbSe CQD surface passivation model, we assign the *d*-spacing to the diffraction of {024} lattice planes with an angle of ~120° relative to the adjacent PbSe {200} lattice fringe (Figure 2e).

Due to the complexity of the Figure 2d, we further apply fast Fourier transform (FFT) to resolve the presence of different crystal spacing indices. Several sets of *d*-spacing indices are extracted from the FFT and inverted FFT patterns (Figure S4): d = 3.7, 3.0, 2.2, and 1.8 Å, which can be assigned to {024} ($(BA)_2PbI_4$), {002} (PbSe), {220} (PbSe), and {311} (PbSe), respectively. A set of indices close to the center (Figure 2f, inset) indicates a periodic pattern with a large *d*-spacing (i.e., 4.1 nm) present. The value is consistent to the average wire-to-wire distance (Figure 2c, inset), and this is confirmed via inverse FFT (Figure S4). The 2D perovskite {024} lattice fringe across the inverse FFT image agrees with the observed presence of bulk 2D perovskite crystal matrix seen in SEM (Figure 2a).

From the above-mentioned analysis, we can propose the following picture of the interface and lattice orientation in the PbSe:2D perovskite hybrids (Figures 3a and S5): The {100}

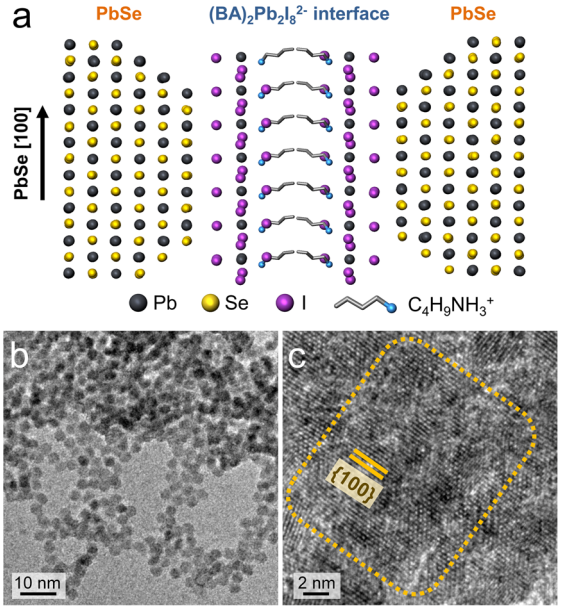

Figure 3. (a) Schematic representation of the interfacial $(BA)_2Pb_2I_8^{2-}$ ligand double layer between two adjacent PbSe nanowires. In the schematic, hydrogen atoms have been omitted for clarity. (b) Bright-field TEM image of drop-cast perovskite-passivated PbSe CQDs (solvent: DMF). (c) High-resolution TEM image of PbSe:perovskite self-assembled heterocrystals showing CQD fusion along [100] crystallographic axes.

facets of PbSe CQDs are passivated by PbI_4^{2-} anions, whose charges are further neutralized by the outer BA^+ ligands; the interdigitation of BA chains during solvent evaporation yields a 2D perovskite-like $(BA)_2Pb_2I_8^{2-}$ double layer with a constant thickness of ~1.4 nm. The latter controls the spacing among the aligned PbSe nanowires within the perovskite matrix.

Solvent selection—the use of butylamine—is key to the formation of hybrid 2D perovskite:PbSe nanowires. When dimethylformamide (DMF) was used instead, only individual PbSe dots are observed (Figure 3b). This observation suggests the $(BA)PbI_4^-$ surface ligand formed by ammonium substitution can readily detach from the PbSe surface during solvent evaporation, producing the fusion of CQDs that yields PbSe nanowires. Detached ligands and free-standing butylamine molecules may further interact with the surfaces of stacked nanowires and ultimately yield the $(BA)_2PbI_4$ 2D perovskite outer shelling seen in SEM. 1D PbSe nanostructure formation via the fusion of PbSe CQDs can be obtained at relatively high temperatures.[14] Spontaneous self-assembly of PbSe CQDs at room temperature leads only to 2D patterns due to the relatively low surface binding energy of PbSe {100} facets.[16,17,32−34] However, in the present case, $(BA)PbI_4^-$ ligand can modulate PbSe fusion to produce 1D self-assembly at room temperature. We do occasionally observe similar 2D type PbSe fusion pattern along {100} facets in some PbSe-rich domains (Figure 3c). It is posited that the formation of this specific 1D PbSe nanowire bundles could be aided by internal dipole moments within PbSe CQDs.[35−38]

In conclusion, the present study demonstrates the self-assembly of PbSe CQDs within a perovskite matrix via *in situ* ligand exchange and solvent evaporation. Surface ammonium substitution by the solvent molecule butylamine creates surface-active facets for CQD fusion and also enables ligand interdigitation among PbSe nanostructures. These joint forces ultimately yield the 1D alignment of PbSe nanowires embedded within a $(BA)_2PbI_4$ 2D perovskite matrix. Future work will investigate further the mechanism of directional fusion, tailor the self-assembled patterns, and explore the electronic properties of these heterocrystals.

■ ASSOCIATED CONTENT

Supporting Information

The Supporting Information is available free of charge on the ACS Publications website at DOI: 10.1021/jacs.5b10641.

Experimental details of PbSe CQD synthesis, perovskite ligand exchange, self-assembly and instrumentation; TEM; STEM-HAADF images of OA-capped PbSe CQDs and PbSe:perovskite hybrids; XRD patterns of $(BA)_2PbI_4$; additional FFT and inverse FFT analyses of Figure 2f; and schematics of the perovskite and PbSe nanowire self-assembled interfaces (PDF)

■ AUTHOR INFORMATION

Corresponding Author

*ted.sargent@utoronto.ca

Author Contributions

‡These authors contributed equally.

Notes

The authors declare no competing financial interest.

■ ACKNOWLEDGMENTS

This publication is based in part on supported by Award KUS-11-009-21, from King Abdullah University of Science and Technology (KAUST), by the Ontario Research Fund-Research Excellence Program, by the Natural Sciences and Engineering Research Council of Canada (NSERC), and by the International Cooperation of the Korea Institute of Energy Technology Evaluation and Planning (KETEP) grant funded by the Korea government Ministry of Knowledge Economy (2012T100100740). A.J. thanks NSERC for Undergraduate Student Research Award Funding. E.Y. acknowledges support from FAPESP-BEPE fellowship (2014/18327-9). The authors thank E. Palmiano, L. Levina, R. Wolowiec, and D. Kopilovic for helpful discussions.

DOI: 10.1021/jacs.5b10641
J. Am. Chem. Soc. XXXX, XXX, XXX−XXX

REFERENCES

(1) Murray, C. B.; Norris, D. J.; Bawendi, M. G. *J. Am. Chem. Soc.* **1993**, *115*, 8706.
(2) Peng, X.; Schlamp, M. C.; Kadavanich, A. V.; Alivisatos, A. P. *J. Am. Chem. Soc.* **1997**, *119*, 7019.
(3) Peng, Z. A.; Peng, X. *J. Am. Chem. Soc.* **2001**, *123*, 183.
(4) Schaller, R. D.; Klimov, V. I. *Phys. Rev. Lett.* **2004**, *92*, 186601.
(5) Peng, X.; Manna, L.; Yang, W.; Wickham, J.; Scher, E.; Kadavanich, A.; Alivisatos, A. P. *Nature* **2000**, *404*, 59.
(6) Kan, S.; Mokari, T.; Rothenberg, E.; Banin, U. *Nat. Mater.* **2003**, *2*, 155.
(7) Wang, J.; Gudiksen, M. S.; Duan, X.; Cui, Y.; Lieber, C. M. *Science* **2001**, *293*, 1455.
(8) Duan, X.; Niu, C.; Sahi, V.; Chen, J.; Parce, J. W.; Empedocles, S.; Goldman, J. L. *Nature* **2003**, *425*, 274.
(9) Cui, Y.; Zhong, Z.; Wang, D.; Wang, W. U.; Lieber, C. M. *Nano Lett.* **2003**, *3*, 149.
(10) Zheng, G.; Patolsky, F.; Cui, Y.; Wang, W. U.; Lieber, C. M. *Nat. Biotechnol.* **2005**, *23*, 1294.
(11) Cui, Y.; Wei, Q.; Park, H.; Lieber, C. M. *Science* **2001**, *293*, 1289.
(12) Tian, B.; Zheng, X.; Kempa, T. J.; Fang, Y.; Yu, N.; Yu, G.; Huang, J.; Lieber, C. M. *Nature* **2007**, *449*, 885.
(13) Bierman, M. J.; Lau, Y. K. A.; Jin, S. *Nano Lett.* **2007**, *7*, 2907.
(14) Cho, K.-S.; Talapin, D. V.; Gaschler, W.; Murray, C. B. *J. Am. Chem. Soc.* **2005**, *127*, 7140.
(15) Arachchige, I. U.; Brock, S. L. *Acc. Chem. Res.* **2007**, *40*, 801.
(16) Williams, K. J.; Tisdale, W. A.; Leschkies, K. S.; Haugstad, G.; Norris, D. J.; Aydil, E. S.; Zhu, X. Y. *ACS Nano* **2009**, *3*, 1532.
(17) Yolanda, J.; Moreels, I.; Karel, L.; Zeger, H. *Nanotechnology* **2010**, *21*, 295606.
(18) Boneschanscher, M. P.; Evers, W. H.; Geuchies, J. J.; Altantzis, T.; Goris, B.; Rabouw, F. T.; van Rossum, S. A. P.; van der Zant, H. S. J.; Siebbeles, L. D. A.; Van Tendeloo, G.; Swart, I.; Hilhorst, J.; Petukhov, A. V.; Bals, S.; Vanmaekelbergh, D. *Science* **2014**, *344*, 1377.
(19) Dolzhnikov, D. S.; Zhang, H.; Jang, J.; Son, J. S.; Panthani, M. G.; Shibata, T.; Chattopadhyay, S.; Talapin, D. V. *Science* **2015**, *347*, 425.
(20) Li, W.; Fan, H.; Li, J. *Nano Lett.* **2014**, *14*, 4951.
(21) Kong, X. Y.; Ding, Y.; Yang, R.; Wang, Z. L. *Science* **2004**, *303*, 1348.
(22) Murray, C. B.; Kagan, C. R.; Bawendi, M. G. *Science* **1995**, *270*, 1335.
(23) Banfield, J. F.; Welch, S. A.; Zhang, H.; Ebert, T. T.; Penn, R. L. *Science* **2000**, *289*, 751.
(24) Dirin, D. N.; Dreyfuss, S.; Bodnarchuk, M. I.; Nedelcu, G.; Papagiorgis, P.; Itskos, G.; Kovalenko, M. V. *J. Am. Chem. Soc.* **2014**, *136*, 6550.
(25) Zhang, H.; Jang, J.; Liu, W.; Talapin, D. V. *ACS Nano* **2014**, *8*, 7359.
(26) Balazs, D. M.; Dirin, D. N.; Fang, H.-H.; Protesescu, L.; ten Brink, G. H.; Kooi, B. J.; Kovalenko, M. V.; Loi, M. A. *ACS Nano* **2015**, DOI: 10.1021/acsnano.5b04547.
(27) Ning, Z.; Gong, X.; Comin, R.; Walters, G.; Fan, F.; Voznyy, O.; Yassitepe, E.; Buin, A.; Hoogland, S.; Sargent, E. H. *Nature* **2015**, *523*, 324.
(28) Yang, Z.; Janmohamed, A.; Lan, X.; Garcia de Arquer, F. P.; Voznyy, O.; Yassitepe, E.; Kim, G.-H.; Ning, Z.; Gong, X.; Comin, R.; Sargent, E. H. *Nano Lett.* **2015**, *15*, 7539.
(29) Mitzi, D. B. *Chem. Mater.* **1996**, *8*, 791.
(30) Cao, D. H.; Stoumpos, C. C.; Farha, O. K.; Hupp, J. T.; Kanatzidis, M. G. *J. Am. Chem. Soc.* **2015**, *137*, 7843.
(31) Yu, W. W.; Falkner, J. C.; Shih, B. S.; Colvin, V. L. *Chem. Mater.* **2004**, *16*, 3318.
(32) Baumgardner, W. J.; Whitham, K.; Hanrath, T. *Nano Lett.* **2013**, *13*, 3225.
(33) Evers, W. H.; Schins, J. M.; Aerts, M.; Kulkarni, A.; Capiod, P.; Berthe, M.; Grandidier, B.; Delerue, C.; van der Zant, H. S. J.; van Overbeek, C.; Peters, J. L.; Vanmaekelbergh, D.; Siebbeles, L. D. A. *Nat. Commun.* **2015**, *6*, 8195.
(34) Baik, S. J.; Kim, K.; Lim, K. S.; Jung, S.; Park, Y.-C.; Han, D. G.; Lim, S.; Yoo, S.; Jeong, S. *J. Phys. Chem. C* **2011**, *115*, 607.
(35) Houtepen, A. J.; Koole, R.; Vanmaekelbergh, D.; Meeldijk, J.; Hickey, S. G. *J. Am. Chem. Soc.* **2006**, *128*, 6792.
(36) Tang, Z.; Zhang, Z.; Wang, Y.; Glotzer, S. C.; Kotov, N. A. *Science* **2006**, *314*, 274.
(37) Talapin, D. V.; Shevchenko, E. V.; Murray, C. B.; Titov, A. V.; Král, P. *Nano Lett.* **2007**, *7*, 1213.
(38) Schliehe, C.; Juarez, B. H.; Pelletier, M.; Jander, S.; Greshnykh, D.; Nagel, M.; Meyer, A.; Foerster, S.; Kornowski, A.; Klinke, C.; Weller, H. *Science* **2010**, *329*, 550.

DOI: 10.1021/jacs.5b10641
J. Am. Chem. Soc. XXXX, XXX, XXX−XXX